Mathematical Modelling and Analysis
Volume 28, Issue 4, 581–595, 2023
https://doi.org/10.3846/mma.2023.18311

Numerical Study of the Equation on the Graph for the Steady State non-Newtonian Flow in Thin Tube Structure

Nikolajus Kozulinas[a], **Grigory Panasenko**[a,b], **Konstantinas Pileckas**[a] **and Vytenis Šumskas**[a]

[a] *Institute of Applied Mathematics, Vilnius University*
Naugarduko g. 24, Vilnius, Lithuania
[b] *Université Jean Monnet*
10 Rue Tréfilerie, Saint-Étienne, France
E-mail: nikolajus.kozulinas@mif.vu.lt
E-mail(*corresp.*): grigory.panasenko@univ-st-etienne.fr
E-mail: konstantinas.pileckas@mif.vu.lt
E-mail: vytenis.sumskas@mif.vu.lt

Received December 15, 2022; accepted October 3, 2023

Abstract. The dimension reduction for the viscous flows in thin tube structures leads to equations on the graph for the macroscopic pressure with Kirchhoff type junction conditions in the vertices. Non-Newtonian rheology of the flow generates nonlinear equations on the graph. A new numerical method for second order nonlinear differential equations on the graph is introduced and numerically tested.

Keywords: non-Newtonian flow, strain rate dependent viscosity, asymptotic dimension reduction, quasi-Poiseuille flows, equation on the graph.

AMS Subject Classification: 35Q35; 76D07.

1 Introduction and main definitions

The Newtonian flows in a network of tubes (tube structures) were considered in [2, 5, 13, 15, 16, 18, 19]. These domains are finite connected unions of thin cylinders (in the two-dimensional case, respectively, thin rectangles). Each tube structure is represented by its graph: if the diameter of cross-sections of cylinders tends to zero, then the tubes degenerate and "tend" to the edges of

the graph. In the case of the stationary Navier-Stokes equations, set in a thin structure, for the pressure one can derive second order ordinary differential equations at the edges of the graph and some Kirchhoff-type junction conditions at the nodes (see [2, 13, 15, 17]). The Kirchhoff junction conditions were introduced for some physiological applications in classical works [10, 11].

In the non-stationary case for the initial-boundary value problem for the Navier-Stokes system, the equation on the graph becomes non-stationary and non-local in time (see [19]). For the periodic in time setting, it was studied in [20]. In [7], a linear stationary equation in an infinite fractal type graph is considered.

Nonlinear equations on the graph are generated by the problems in thin tube structures for viscous flows with non-Newtonian rheology. The case of the Stokes equations with the shear rate dependent viscosity was considered in the set of three papers [21, 22, 23], where the complete asymptotic expansion of the solution was constructed (also see [3, 4] for the Bingham law rheology and [9] for the power law rheology). In particular, in [22] a nonlinear equation on the graph is studied. Its unknown function is the macroscopic pressure in the network of thin pipes. This problem is crucial for the construction of asymptotic approximations of the solution of the Stokes type equation in tube structures because it gives the leading term. These problems on the graph need fast effective solvers. The present paper introduces a new numerical method of its solution, formulates the convergence theorem and provides numerical tests.

Other one-dimension models for the blood flow applications were derived from the general conservation laws in [6, 12, 25].

2 Thin tube structure and its graph

For the reader's convenience we remind the definitions of the tube structure and its graph given in [13].

Definition 1. Let $O_1, O_2, ..., O_N$ be N different points in $\mathbb{R}^n, n = 2, 3$, and $e_1, e_2, ..., e_M$ be M closed segments each connecting two of these points (i.e., each $e_j = \overline{O_{i_j} O_{k_j}}$, where $i_j, k_j \in \{1, ..., N\}, i_j \neq k_j$). All points O_i are supposed to be the ends of some segments e_j. The segments e_j are called edges of the graph. A point O_i is called a node, if it is the common end of at least two edges, and O_i is called a vertex, if it is the end of the only one edge. Any two edges e_j and e_i can intersect only at the common node. The set of vertices is supposed to be non-empty.

Denote $\mathcal{B} = \cup_{j=1}^{M} e_j$ the union of edges and assume that $\mathcal{B}$ is a connected set. The graph $\mathcal{G}$ is defined as the collection of nodes, vertices and edges (see Figure 1).

Let e be some edge, $e = \overline{O_i O_j}$. Consider two Cartesian coordinate systems in $\mathbb{R}^n$. The first one has the origin in O_i and the axis $O_i x_1^{(e)}$ has the direction of the ray $[O_i O_j)$; the second one has the origin in O_j and the opposite direction, i.e. $O_i \tilde{x}_1^{(e)}$ is directed over the ray $[O_j O_i)$.

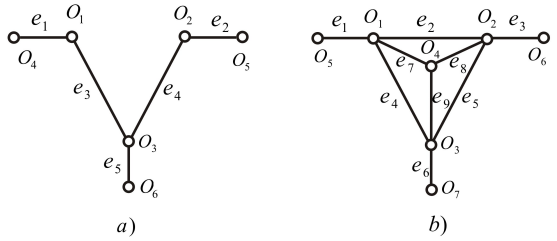

Figure 1. Graphs of tube structure.

Below, in various situations we choose one or another coordinate system denoting the local variable in both cases by $x^{(e)}$ and pointing out which end is taken as the origin of the coordinate system.

With every edge e_j we associate a bounded domain $\sigma^j \subset \mathbb{R}^{n-1}$ containing the origin O and having C^4-smooth boundary $\partial\sigma^j, j = 1, ..., M$. For every edge $e_j = e$ and associated $\sigma^j = \sigma^{(e)}$ we denote by $\sigma_\varepsilon^{(e)}$ the set $\{x^{(e)\prime} \in \mathbb{R}^{n-1} : x^{(e)\prime}/\varepsilon \in \sigma^{(e)}\}$, and by $\Pi_\varepsilon^{(e)}$ the cylinder ("tube")

$$\Pi_\varepsilon^{(e)} = \Big\{x^{(e)} \in \mathbb{R}^n : x_1^{(e)} \in (0, |e|), x^{(e)\prime}/\varepsilon \in \sigma^{(e)}\Big\},$$

where $x^{(e)\prime} = (x_2^{(e)}, ..., x_n^{(e)})$, $|e|$ is the length of the edge e and $\varepsilon > 0$ is a small parameter. Notice that the edges e_j and Cartesian coordinates of nodes and vertices O_j, as well as the domains σ_j, do not depend on ε.

Let $O_1, ..., O_{N_1}$ be nodes and $O_{N_1+1}, ..., O_N$ be vertices. Let $\omega^1, ..., \omega^N$ be bounded independent of ε domains in $\mathbb{R}^n$; introduce the nodal domains $\omega_\varepsilon^j = \{x \in \mathbb{R}^n : \frac{x-O_j}{\varepsilon} \in \omega^j\}$.

Definition 2. By a tube structure we call the following domain (see Figure 2)

$$B_\varepsilon = \Big(\bigcup_{j=1}^{M} \Pi_\varepsilon^{(e_j)}\Big) \bigcup \Big(\bigcup_{j=1}^{N} \omega_\varepsilon^j\Big).$$

Suppose that it is a connected set and that the boundary ∂B_ε of B_ε is C^4-smooth.

The fourth order smoothness of the boundary is required to prove the existence of the solution to the non-Newtonian problem, see [23].

Consider a node or a vertex O_l and all edges e_j having O_l as one of their end points. We call a bundle of edges $\mathcal{B}_l$ the union of all these edges, i.e., $\mathcal{B}_l = \cup_{j:O_l \in e_j} e_j$.

3 Motivation: a non-Newtonian flow in network of tubes

Let $n = 2, 3$, $\nu_0, \lambda > 0$ be positive constants. Let ν be a bounded C^3-smooth function $\mathbb{R}^{n(n+1)/2} \to \mathbb{R}$ such that for all $y \in \mathbb{R}^{n(n+1)/2}$,

$$|\nu(y)| \le C, \ |\nabla^\beta \nu(y)| \le C, \ \beta = 1, 2, 3,$$

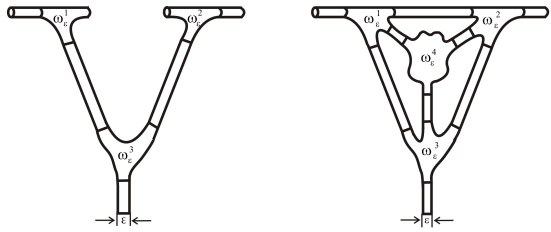

Figure 2. Fluid flow tube structure.

where C is a positive constant.

In the tube structure B_ε, consider the steady state boundary value problem for the non-Newtonian fluid motion equations

$$\begin{cases} -\mathrm{div}((\nu_0 + \lambda\nu(\dot\gamma(\mathbf{v}))D(\mathbf{v})) + \nabla p = 0, \quad x \in B_\varepsilon, \\ \mathrm{div}\mathbf{v} = 0, \quad \mathrm{x} \in \mathrm{B}_\varepsilon, \\ \mathbf{v}|_{\partial B_\varepsilon} = \varepsilon\mathbf{g}, \end{cases} \tag{3.1}$$

where $D(\mathbf{v})$ is the strain rate matrix with the elements $d_{ij} = \frac{1}{2}(\frac{\partial v_i}{\partial x_j} + \frac{\partial v_j}{\partial x_i})$, $\dot\gamma(\mathbf{v}) = (d_{12}, d_{13}, d_{23}, d_{11}, d_{22}, d_{33})$ if $n = 3$ and $\dot\gamma(\mathbf{v}) = (d_{12}, d_{11}, d_{22})$ if $n = 2$.

Assume that the fluid velocity $\mathbf{g}$ at the boundary ∂B_ε has the following structure: $\mathbf{g} = 0$ everywhere on ∂B_ε except for the set $\gamma_\varepsilon^{N_1+1}, ..., \gamma_\varepsilon^N$, where $\gamma_\varepsilon^j = \partial B_\varepsilon \cap \partial\omega_\varepsilon^j$, $j = N_1 + 1, \ldots, N$, i.e.,

$$\mathbf{g}(x)|_{\gamma_\varepsilon^j} = \mathbf{g}^j\left((x - O_j)/\varepsilon\right)\big|_{\gamma_\varepsilon^j}, \quad j = N_1 + 1, ..., N,$$
$$\mathbf{g}(x,t)\big|_{\partial B_\varepsilon \setminus (\cup_{j=N_1+1}^N \gamma_\varepsilon^j)} = 0,$$

where $\mathbf{g}^j \in H^{5/2}(\gamma^j)$, $\gamma^j = \varepsilon^{-1}(\gamma_\varepsilon^j - O_j)$ the corresponding dilated part of the boundary, $\mathbf{g} \in H^{5/2}(\partial B_\varepsilon)$.

Let $e = e_{O_j}$ be the edge with the end at the vertex O_j and let $x^{(e)}$ be the Cartesian coordinates corresponding to the origin O_j and the edge e, i.e., $x^{(e)} = \mathcal{P}^{(e)}(x - O_j)$, $\mathcal{P}^{(e)}$ is the orthogonal matrix relating the global coordinates x with the local ones $x^{(e)}$. Denote $\mathbf{g}^{(e)} = \mathcal{P}^{(e)}\mathbf{g}^j$.

Let

$$F_\varepsilon^j = \varepsilon\int_{\gamma_\varepsilon^j} \mathbf{g}(x)\cdot\mathbf{n}(x)\mathrm{d}S = \varepsilon\int_{\gamma_\varepsilon^j} \mathbf{g}^j\left((x - O_j)/\varepsilon\right)\cdot\mathbf{n}(x)\mathrm{d}S$$
$$= \varepsilon^n\int_{\gamma^j} \hat{\mathbf{g}}_n^j(y^{(e)'})\mathrm{d}y^{(e)'} = \varepsilon^n F_j, \quad j = N_1 + 1, ..., N,$$

where $\mathbf{n}$ is the unit outward (with respect to B_ε) normal vector to γ_ε^j, $y^{(e)} = x^{(e)}/\varepsilon$, $\hat{\mathbf{g}}^j(y^{(e)}) = \mathbf{g}^j((\mathcal{P}^{(e)})^T y^{(e)})$ (here "T" denotes the transposition), F_j does not depend on ε. Assume the compatibility condition for the flow rates F_j: $\sum_{j=1}^J F_j = 0$.

An asymptotic analysis of this problem with small parameter ε leads to a nonlinear elliptic problem on the graph [21,22,23]. The solution of this problem determines the leading term of the pressure in problem (3.1).

Let us introduce this problem on the graph.

4 Equation on the graph

For any edge e with associated cross-section $\sigma_\varepsilon^{(e)}$ we introduce a function $\mathcal{F}_{\sigma_\varepsilon^{(e)}}$ such that

$$\mathcal{F}_{\sigma_\varepsilon^{(e)}}(\alpha) = \int_{\sigma_\varepsilon^{(e)}} v_{P_\alpha}(x')\mathrm{d}x',$$

where v_{P_α} is a solution of the boundary value problem

$$\begin{cases} -\frac{1}{2}\mathrm{div}_{x'}\big((\nu_0 + \lambda\nu(\dot\gamma_P(v_{P_\alpha})))\nabla_{x'}v_{P_\alpha}\big) = \alpha, \quad x' \in \sigma_\varepsilon^{(e)}, \\ v_{P_\alpha}|_{\partial\sigma_\varepsilon^{(e)}} = 0. \end{cases} \tag{4.1}$$

If $\lambda = 0$ then $\mathcal{F}_{\sigma_\varepsilon^{(e)}}$ is a linear function, equal to $\kappa_{\sigma_\varepsilon^{(e)}}\alpha$, where $\kappa_{\sigma_\varepsilon^{(e)}}$ is a positive constant. For any λ denote $\mathcal{G}_{\sigma_\varepsilon^{(e)}}(\alpha) = \mathcal{F}_{\sigma_\varepsilon^{(e)}}(\alpha) - \kappa_{\sigma_\varepsilon^{(e)}}\alpha$.

Here $\dot\gamma_P(v_{P_\alpha})=(\frac{1}{2}\nabla_{x'}v_{P_\alpha}, 0, 0)$ if n=2, $\dot\gamma_P(v_{P_\alpha})=(\frac{1}{2}\nabla_{x'}v_{P_\alpha}, 0, 0, 0, 0)$ if n=3, and α is a given pressure slope. In what follows, we omit the subscript ε.

With the above notations, consider the following problem on the graph $\mathcal{B}$: given constants F_l, $l = N_1+1, ..., N$, such that $\sum_{l=N_1+1}^{N} F_l = 0$ and constants c_{lj}, $l = 1, ..., N_1$, (here, for any l subscript, j is such that the edges e_j have an end point O_l), find a function p which is affine with respect to $x_1^{(e_j)}$,

$$p(x_1^{(e_j)}) = -\alpha_j x_1^{(e_j)} + a_j,$$

such that

$$\begin{cases} \dfrac{\partial}{\partial x_1^{(e_j)}}\Big(\mathcal{F}_{\sigma_j}(-\dfrac{\partial p}{\partial x_1^{(e_j)}}(x_1^{(e_j)}))\Big) = 0, \quad x_1^{(e_j)} \in (0, |e_j|), \\ \sum\limits_{e_j : O_l \in e_j} \mathcal{F}_{\sigma_j}(-\dfrac{\partial p}{\partial x_1^{(e_j)}}(0)) = 0, \quad l = 1, ..., N_1, \\ \mathcal{F}_{\sigma_j}(-\dfrac{\partial p}{\partial x_1^{(e_j)}}(0)) = -F_l, \quad l = N_1+1, ..., N, \quad O_l \in e_j, \\ p(x_1^{(e_j)} = 0) - p(x_1^{(e_s)} = 0) = c_{lj}, \quad e_j : O_l \in e_j, \ l = 1, ..., N_1, \\ p(O_N) = 0. \end{cases} \tag{4.2}$$

The fourth condition means that the solution p may have prescribed jumps c_{lj} at the nodes $O_l \in e_j$, $l = 1, ..., N_1$, so that for a fixed node O_l at the ends of different edges e_j (when the local variable $x_1^{(e_j)}$ is equal to 0) the solution p has its value which differs from the value of p at the end of the selected edge e_s and the difference is equal to c_{lj}. For the leading term $c_{lj} = 0$, and so p is continuous on the graph. However for the further terms c_{lj} may be different from zero.

Remark 1. In [21, 22, 23] it is proved that for any $\alpha_0 > 0, C > 0$ there exists $\lambda_0 > 0$ such that for $|\lambda| \le \lambda_0$, $C\mathcal{G}_{\sigma^{(e)}}$ is a contraction on the interval $[-\alpha_0, \alpha_0]$, and there exists a solution to (4.2), unique in some ball $B_R = \{q \in$

$\mathcal{H}_{O_N}(\mathcal{B}), \|q\|_{\mathcal{H}(\mathcal{B})} \le R\}$. Here $\mathcal{H}(\mathcal{B})$ is the space of functions defined on the graph, belonging to $H^1(e_j)$ on every edge e_j of the graph, and $\mathcal{H}_{O_N}(\mathcal{B})$ is the subspace of functions from $\mathcal{H}(\mathcal{B})$ vanishing at O_N; the space $\mathcal{H}(\mathcal{B})$ is supplied with the norm defined by the relation:

$$\|q\|^2_{\mathcal{H}(\mathcal{B})} = \sum_{j=1}^{M} \|q\|^2_{H^1(e_j)}.$$

We will also consider the subspaces $H^1(\mathcal{B})$ of $\mathcal{H}(\mathcal{B})$ and $H^1_{O_N}(\mathcal{B})$ of $\mathcal{H}_{O_N}(\mathcal{B})$ consisting of continuous on $\mathcal{B}$ functions, without gaps at the nodes.

The proof of the existence of the solution to problem (4.2) is based on the fixed point method applied in some ball B_R in the space $\mathcal{H}(\mathcal{B})$. Every iteration is related to the following linear problem.

For $f_0^{(e_j)}, f_1^{(e_j)} \in L^2(e_j)$, find $p \in \mathcal{H}(\mathcal{B})$ such that

$$\begin{cases} -\dfrac{\partial}{\partial x_1^{(e_j)}}\Big(\kappa_{\sigma_j}\big(\dfrac{\partial p}{\partial x_1^{(e_j)}}(x_1^{(e_j)})\big)\Big) = f_0^{(e_j)} - \dfrac{\partial f_1^{(e_j)}}{\partial x_1^{(e_j)}}, \quad x_1^{(e_j)} \in (0, |e_j|), \\ -\sum\limits_{e_j : O_l \in e_j} \kappa_{\sigma_j}\big(\dfrac{\partial p}{\partial x_1^{(e_j)}}(0)\big) = -\sum\limits_{e_j : O_l \in e_j} f_1^{(e_j)}(0), \quad l = 1, ..., N_1, \\ -\kappa_{\sigma_j}\big(\dfrac{\partial p}{\partial x_1^{(e_j)}}(0)\big) = -F_l - f_1^{(e_j)}(0), \quad l = N_1+1, ..., N, \quad O_l \in e_j, \\ p(x_1^{(e_j)} = 0) - p(x_1^{(e_s)} = 0) = c_{lj}, \quad e_j : O_l \in e_j, \ l = 1, ..., N_1, \\ p(O_N) = 0. \end{cases} \tag{4.3}$$

Let us describe a change of the unknown function p which allows to reduce problem (4.3) to a problem of the same type but for an unknown function continuous on the graph. Let ζ be a C^3-smooth function defined on $[0, +\infty)$ equal to zero on $[0, 1/6]$ and equal to one on $[1/3, +\infty)$. Introducing on every edge e_j function $\big(1 - \zeta\big(x_1^{(e_j)}/|e_j|\big)\big)c_{lj}$ we change the unknown function p on the edge e_j $(j \ne s)$ by $\tilde{p} = p - \big(1 - \zeta\big(x_1^{(e_j)}/|e_j|\big)\big)c_{lj}$. We get for the new unknown function $\tilde{p}^{(e)}$. Equation (4.3) with new right-hand sides

$$\tilde{f}^{(e_j)}(x_1^{(e_j)}) = f_0^{(e_j)}(x_1^{(e_j)}) - \frac{\partial f_1^{(e_j)}}{\partial x_1^{(e_j)}}(x_1^{(e_j)}) - \kappa_{\sigma_j}|e_j|^{-2}\zeta''\Big(\frac{x_1^{(e_j)}}{|e_j|}\Big)c_{lj}.$$

Function $\tilde{p}$ is continuous on $\mathcal{B}$ and satisfies the following variational formulation:

$$\begin{aligned} &\sum_{j=1}^{M} \int_0^{|e_j|} \kappa_{\sigma_j}\big(\frac{\partial \tilde{p}}{\partial x_1^{(e_j)}}(x_1^{(e_j)})\big)\frac{\partial q}{\partial x_1^{(e_j)}}\mathrm{d}x_1^{(e_j)} + \sum_{l=N_1+1}^{N} F_l\, q(O_l) \\ &\quad = \sum_{j=1}^{M} \int_0^{|e_j|} \big(\tilde{f}_0^{(e_j)}(x_1^{(e_j)})q(x_1^{(e_j)}) + f_1^{(e_j)}(x_1^{(e_j)})\frac{\partial q}{\partial x_1^{(e_j)}}\big)\mathrm{d}x_1^{(e_j)} \end{aligned} \tag{4.4}$$

for all $q \in H^1_{O_N}(\mathcal{B})$. Here

$$\tilde{f}_0^{(e_j)}(x_1^{(e_j)}) = f_0^{(e_j)}(x_1^{(e_j)}) - \kappa_{\sigma_j}|e_j|^{-2}\zeta''\big(x_1^{(e_j)}/|e_j|\big)c_{lj}.$$

It is supposed that the following compatibility condition holds:

$$\sum_{i=1}^{M}\int_{0}^{|e_i|} f_0^{(e_i)}\mathrm{d}x_n^{(e_i)} + \sum_{l=N_1+1}^{N} F_l = 0.$$

Treating the left-hand side of (4.4) as an inner product in the space $H^1_{O_N}(\mathcal{B})$ and its right-hand side as a bounded linear functional we apply the Riesz theorem and prove that this problem admits a unique solution. Moreover, taking the test function $q = \tilde{p}$ and applying the Cauchy-Buniakovsky-Schwarz inequality, we prove that there exists a constant $C_{\mathcal{B}}$ depending on $\mathcal{B}$ only, such that

$$\begin{aligned}\|p\|_{\mathcal{H}(\mathcal{B})} \le & C_{\mathcal{B}}\Big(\|\tilde{f}_0\|_{L^2(\mathcal{B})} + \|\tilde{f}_1\|_{L^2(\mathcal{B})} \\ & + \sum_{i=1}^{N_1}\sum_{j:e_j:O_l\in e_j;e_j=e_{j_s}} |c_{ij}| + \Big(\sum_{l=N_1+1}^{N-1}|F_l|^2\Big)^{1/2}\Big). \end{aligned} \tag{4.5}$$

For more details, see [17].

Remark 2. Note that if for any edge e, $f_0^{(e)} = 0$ and $f_1^{(e)} = const$, then on each edge e the solution p is an affine function.

5 Iterative methods to solve the equation on the graph

5.1 Classical fixed point method

Denote by $\mathcal{H}_L(\mathcal{B})$ the subspace of $\mathcal{H}(\mathcal{B})$ consisting of functions linear at every edge e. Consider the mapping $\tilde{\mathcal{L}}$: $\mathcal{H}_L(\mathcal{B}) \cap B_R \to \mathcal{H}_L(\mathcal{B})$ such that $\tilde{\mathcal{L}}p$ is a solution of the linear problem on the graph:

$$\begin{cases} -\kappa_j \dfrac{\partial^2 \tilde{\mathcal{L}}p}{\partial x_1^{(e_j)2}} = -\dfrac{\partial}{\partial x_1^{(e_j)}}\Big(\mathcal{G}_{\sigma_j}(-\dfrac{\partial p}{\partial x_1^{(e_j)}}(x_1^{(e_j)}))\Big), \quad x_1^{(e_j)} \in (0, |e_j|), \\ -\sum\limits_{e_j:O_l\in e_j} \kappa_j \dfrac{\partial \tilde{\mathcal{L}}p}{\partial x_1^{(e_j)}}(0) = -\sum\limits_{e_j:O_l\in e_j} \mathcal{G}_{\sigma_j}(-\dfrac{\partial p}{\partial x_1^{(e_j)}}(0)), \quad l = 1, ..., N_1, \\ -\kappa_j \dfrac{\partial \tilde{\mathcal{L}}p}{\partial x_1^{(e_j)}}(0) = -\mathcal{G}_{\sigma_j}(-\dfrac{\partial p}{\partial x_1^{(e_j)}}(0)) - F_l, \quad l = N_1+1, ..., N, \quad O_l \in e_j, \\ \tilde{\mathcal{L}}p(x_1^{(e_j)} = 0) - \tilde{\mathcal{L}}p(x_1^{(e_s)} = 0) = c_{lj}, \quad e_j : O_l \in e_j, \ l = 1, ..., N_1, \\ \tilde{\mathcal{L}}p(O_N) = 0. \end{cases}$$

This problem is an elementary iteration to solve problem (4.2).

Applying Remark 1, we get that there exists λ_0 such that for all $|\lambda| \le \lambda_0$, $\tilde{\mathcal{L}}$ is a contraction in $\mathcal{H}_L(\mathcal{B}) \cap B_R$. Therefore, problem (4.2) can be solved by the fixed point iterations converging for any initial approximation from B_R, for

example, $p^0 = 0$. The iterations are defined as follows: $p^{k+1} = \tilde{\mathcal{L}} p^k$, i.e.,

$$\begin{cases} -\kappa_j \dfrac{\partial^2 p^{k+1}}{\partial x_1^{(e_j)2}} = -\dfrac{\partial}{\partial x_1^{(e_j)}}\Big(\mathcal{G}_{\sigma_j}(-\dfrac{\partial p^k}{\partial x_1^{(e_j)}}(x_1^{(e_j)}))\Big), \quad x_1^{(e_j)} \in (0, |e_j|), \\ -\sum\limits_{e_j : O_l \in e_j} \kappa_j \dfrac{\partial p^{k+1}}{\partial x_1^{(e_j)}}(0) = -\sum\limits_{e_j : O_l \in e_j} \mathcal{G}_{\sigma_j}(-\dfrac{\partial p^k}{\partial x_1^{(e_j)}}(0)), \quad l = 1, ..., N_1, \\ -\kappa_j \dfrac{\partial p^{k+1}}{\partial x_1^{(e_j)}}(0) = -\mathcal{G}_{\sigma_j}(-\dfrac{\partial p^k}{\partial x_1^{(e_j)}}(0)) - F_l, \quad l = N_1 + 1, ..., N, \quad O_l \in e_j, \\ p^{k+1}(x_1^{(e_j)} = 0) - p^{k+1}(x_1^{(e_s)} = 0) = c_{lj}, \quad e_j : O_l \in e_j, \ l = 1, ..., N_1, \\ p^{k+1}(O_N) = 0. \end{cases} \tag{5.1}$$

Each piecewise-affine function $p \in \mathcal{H}_L(\mathcal{B}) \cap B_R$ is in one-to-one correspondence with the set of values of p in the ends of the edges e, so that (5.1) is equivalent to a linear system of equations with inversible matrix $\mathcal{M}$. So, it can be solved by applying the LU-factorization of $\mathcal{M}$ (calculated only once for the whole chain of iterations) and then solving the two standard triangular systems of equations at each step of iterations. However, for large N and sparse matrix $\mathcal{M}$, the GMRES method for each iteration may be more effective.

5.2 Fixed point method with preconditioner

Consider a more robust iterative method: given a positive number τ (further called "artificial time"), calculate recurrently

$$\begin{cases} -\kappa_j \dfrac{\partial^2 (p^{k+1} - p^k)}{\partial x_1^{(e_j)2}} = -\tau \dfrac{\partial}{\partial x_1^{(e_j)}}\Big(\mathcal{F}_{\sigma_j}(-\dfrac{\partial p^k}{\partial x_1^{(e_j)}}(x_1^{(e_j)}))\Big), \quad x_1^{(e_j)} \in (0, |e_j|), \\ -\sum\limits_{e_j : O_l \in e_j} \kappa_j \dfrac{\partial (p^{k+1} - p^k)}{\partial x_1^{(e_j)}}(0) = -\tau \sum\limits_{e_j : O_l \in e_j} \mathcal{F}_{\sigma_j}(-\dfrac{\partial p^k}{\partial x_1^{(e_j)}}(0)), \quad l = 1, ..., N_1, \\ -\kappa_j \dfrac{\partial (p^{k+1} - p^k)}{\partial x_1^{(e_j)}}(0) = -\tau(\mathcal{F}_{\sigma_j}(-\dfrac{\partial p^k}{\partial x_1^{(e_j)}}(0)) + F_l), l = N_1 + 1, ..., N, O_l \in e_j, \\ p^{k+1}(x_1^{(e_j)} = 0) - p^{k+1}(x_1^{(e_s)} = 0) = c_{lj}, \quad e_j : O_l \in e_j, \ l = 1, ..., N_1, \\ p^{k+1}(O_N) = 0. \end{cases} \tag{5.2}$$

Let us analyse for what values of τ this method converges. Let λ be a positive constant such that $C_{\mathcal{B}} \mathcal{G}_{\sigma^{(e)}}$ is a contraction with factor ρ. Let p be the exact solution of problem (4.2). Then, evidently, the difference $q^k = p^k - p$ is a solution of the problem

$$\begin{cases} -\kappa_j \dfrac{\partial^2 (q^{k+1} - q^k)}{\partial x_1^{(e_j)2}} = -\tau \dfrac{\partial}{\partial x_1^{(e_j)}}\Big(\mathcal{F}_{\sigma_j}(-\dfrac{\partial p^k}{\partial x_1^{(e_j)}}(x_1^{(e_j)})) - \mathcal{F}_{\sigma_j}(-\dfrac{\partial p}{\partial x_1^{(e_j)}}(x_1^{(e_j)}))\Big), \\ x_1^{(e_j)} \in (0, |e_j|), \\ -\sum\limits_{e_j : O_l \in e_j} \kappa_j \dfrac{\partial (q^{k+1} - q^k)}{\partial x_1^{(e_j)}}(0) = -\tau \sum\limits_{e_j : O_l \in e_j} \Big(\mathcal{F}_{\sigma_j}(-\dfrac{\partial p^k}{\partial x_1^{(e_j)}}(0)) - \mathcal{F}_{\sigma_j}(-\dfrac{\partial p}{\partial x_1^{(e_j)}}(0))\Big), \end{cases}$$

$$\begin{cases} l=1,...,N_1, \\ -\kappa_j \dfrac{\partial(q^{k+1}-q^k)}{\partial x_1^{(e_j)}}(0) = -\tau\Big(\mathcal{F}_{\sigma_j}(-\dfrac{\partial p^k}{\partial x_1^{(e_j)}}(0)) - \mathcal{F}_{\sigma_j}(-\dfrac{\partial p}{\partial x_1^{(e_j)}}(0))\Big), \\ l=N_1+1,...,N, \quad O_l \in e_j, \\ q^{k+1}(x_1^{(e_j)}=0) - q^{k+1}(x_1^{(e_s)}=0) = 0, \quad e_j : O_l \in e_j,\ l=1,...,N_1, \\ q^{k+1}(O_N)=0, \end{cases}$$

i.e.,

$$\begin{cases} -\kappa_j \dfrac{\partial^2(q^{k+1}-(1-\tau)q^k)}{\partial x_1^{(e_j)2}} = -\tau \dfrac{\partial}{\partial x_1^{(e_j)}}\Big(\mathcal{G}_{\sigma_j}(-\dfrac{\partial p^k}{\partial x_1^{(e_j)}}(x_1^{(e_j)})) \\ \quad -\mathcal{G}_{\sigma_j}(-\dfrac{\partial p}{\partial x_1^{(e_j)}}(x_1^{(e_j)}))\Big), \quad x_1^{(e_j)} \in (0,|e_j|), \\ -\sum\limits_{e_j:O_l\in e_j} \kappa_j \dfrac{\partial(q^{k+1}-(1-\tau)q^k)}{\partial x_1^{(e_j)}}(0) = -\tau \sum\limits_{e_j:O_l\in e_j} \Big(\mathcal{G}_{\sigma_j}(-\dfrac{\partial p^k}{\partial x_1^{(e_j)}}(0)) \\ \quad -\mathcal{G}_{\sigma_j}(-\dfrac{\partial p}{\partial x_1^{(e_j)}}(0))\Big), \quad l=1,...,N_1, \\ -\kappa_j \dfrac{\partial(q^{k+1}-(1-\tau)q^k)}{\partial x_1^{(e_j)}}(0) = -\tau\Big(\mathcal{G}_{\sigma_j}(-\dfrac{\partial p^k}{\partial x_1^{(e_j)}}(0)) - \mathcal{G}_{\sigma_j}(-\dfrac{\partial p}{\partial x_1^{(e_j)}}(0))\Big), \\ l=N_1+1,...,N, \quad O_l \in e_j, \\ (q^{k+1}-(1-\tau)q^k)(x_1^{(e_j)}=0) - (q^{k+1}-(1-\tau)q^k)(x_1^{(e_s)}=0) = 0, \\ e_j : O_l \in e_j,\ l=1,...,N_1, \\ (q^{k+1}-(1-\tau)q^k)(O_N)=0. \end{cases}$$

Applying for $q^{k+1}-(1-\tau)q^k$ the estimate (4.5) and taking into consideration that $C_{\mathcal{B}}\mathcal{G}$ is a contraction with the contraction factor ρ, we get

$$\begin{aligned} \|q^{k+1}-(1-\tau)q^k\|_{\mathcal{H}(\mathcal{B})} \le & C_{\mathcal{B}}\tau \|\mathcal{G}_{\sigma_j}(-\frac{\partial p^k}{\partial x_1^{(e_j)}}(x_1^{(e_j)})) - \mathcal{G}_{\sigma_j}(-\frac{\partial p}{\partial x_1^{(e_j)}}(x_1^{(e_j)}))\|_{L^2(\mathcal{B})} \\ \le & \rho\tau \|q^k\|_{L^2(\mathcal{B})}. \end{aligned}$$

Therefore,

$$\|q^{k+1}\|_{\mathcal{H}(\mathcal{B})} \le (1-\tau)\|q^k\|_{\mathcal{H}(\mathcal{B})} + \tau\rho\|q^k\|_{\mathcal{H}(\mathcal{B})}.$$

Note that for sufficiently small λ, we have $\rho < 1$. In this case, sequence (5.2) converges to the exact solution to problem (4.2) due to Banach's fixed point theorem.

The choice of parameter τ can be optimized to ensure the fastest convergence rate if some additional information on the spectrum of the linearized problem is known (see, for instance, [1], Chapter VI; [26], Section 5.8; or [14], Section 1.1.1).

6 Numerical experiments

To illustrate the implementation of the iterative method and to test its accuracy, it was investigated for two graph examples. To describe the flow, we

consider a real life blood rheology corresponding to the non-Newtonian Carreau law [8]

$$\nu_0 + \lambda\nu(\dot\gamma) = 0.00345 + 0.05255(1 + (3.313\dot\gamma)^2)^{-0.3216}\ \text{Pa}\cdot\text{s}.$$

To define the function $\mathcal{F}_{\sigma_\varepsilon^{(e)}}(\alpha)$, we assume that the cylinders of the tube structure have a round shape of cross-sections, so that $\sigma_\varepsilon^{(e)}$ is a disk. To get this relation, one should solve problem (4.1) for all α on the cross-section of each tube. Instead, we provided the direct COMSOL 3D simulation of the non-Newtonian flow through a cylindric tube of the length 0.1 m and diameter 0.01 m for a set of values of α. On the lateral boundary of the cylinder, the no-slip boundary condition was set, while on the inflow and outflow the normal velocity corresponding to the given flux was defined. We found out that $\mathcal{F}_{\sigma_\varepsilon^{(e)}}(\alpha)$ can be approximated as follows:

$$\mathcal{F}_\sigma(\alpha) = 3.3372\cdot 10^{-10}\cdot\alpha^{1.4164}\text{m}^3/\text{s}.$$

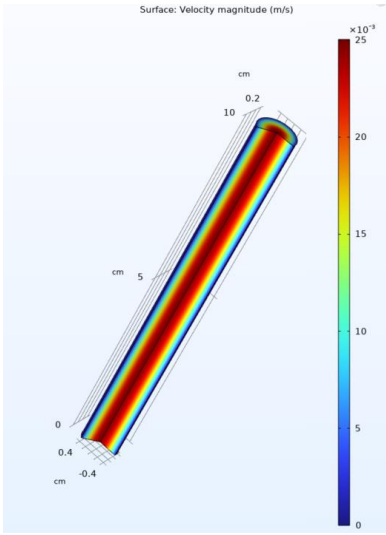

Figure 3. Level surfaces of the velocity in a tube.

In Figure 3, one can see that the level surfaces of the velocity are parallel everywhere except for the small zones near the bases of the cylinder (boundary layer zones). The smallness of the boundary layer zones confirms the asymptotic analysis developed in [23] in the case when the thin tube structure is presented by one thin cylinder. According to this analysis on the cross-section in the middle of the tube, we obtain the solution of the corresponding problem (4.1). Figure 4 shows the computed relation between the flux and the pressure slope for several values of the pressure slope.

To fit it for a tube σ_ε with diameter equal to 0.01ε m, the following property (see [22]) is employed:

$$\mathcal{F}_{\sigma_\varepsilon}(x) = \varepsilon^n\mathcal{F}_\sigma(\varepsilon x).$$

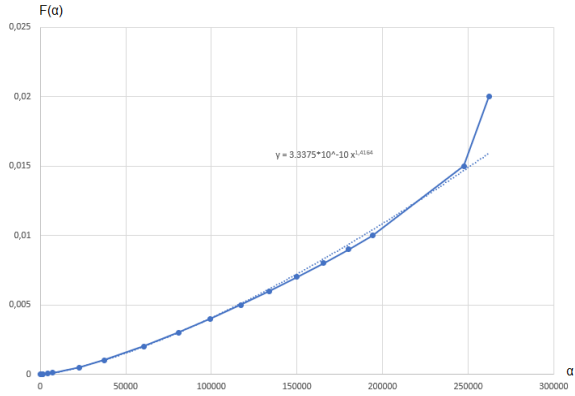

Figure 4. Curve flux/pressure slope. Continuous line corresponds to the interpolation, while the dashed line is defined by the least square method.

6.1 A simple graph example

First, the iterative algorithm was tested for a model example pictured in Figure 5.

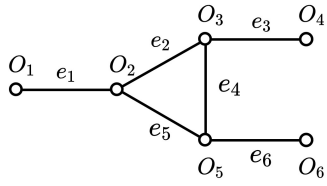

Figure 5. First graph example with 6 nodes/vertices O_i and 6 edges e_j.

The diameters of the vessels are assumed to be equal to 10^{-3} m and their lengths to 10^{-2} m. For realistic fluxes, the following boundary conditions are used: $F_1^\varepsilon = -3.75 \cdot \pi \cdot 10^{-8}$, $F_4^\varepsilon = 1.25 \cdot \pi \cdot 10^{-8}$, $F_6^\varepsilon = 2.5 \cdot \pi \cdot 10^{-8}$, $F_2^\varepsilon = F_3^\varepsilon = F_5^\varepsilon = 0$.

Table 1 below shows values of nodes/vertices O_i computed with the iterative algorithm. An exact solution is presented as well, which was found using the MATLAB nonlinear equations solver *Fsolve*. Note that these results are subject to one predetermined unknown (O_1 in this case), which is required for a unique solution to exist.

6.2 A realistic graph example

Next, the iterative algorithm was tested on a realistic graph of blood vessels. A segment of network from [24] was used with realistic lengths, while the diameters were simplified to all equal 10^{-4} m. Figure 6 below depicts the graph of this vessel network.

Table 1. Values of graph points O_i for the first example. The "Exact" line gives the solution found with MATLAB nonlinear equations solver *Fsolve*, while others show results acquired with the proposed iterative method. Here, equations were scaled by 10^{10} and for the optimal convergence rate, the step size in artificial time was taken equal to 1/22.

	O_1	O_2	O_3	O_4	O_5	O_6
Exact	0	6.2919	9.6323	12.5292	10.6382	15.3639
Iteration 1	0	5.3550	7.7350	9.5200	8.3300	11.9000
Iteration 2	0	6.4484	9.7529	12.4238	10.6490	15.3893
Iteration 3	0	6.2588	9.6151	12.4800	10.5902	15.3149
Iteration 4	0	6.2987	9.6445	12.5373	10.6412	15.3669
Iteration 5	0	6.2906	9.6326	12.5289	10.6357	15.3613
Iteration 6	0	6.2922	9.6331	12.5299	10.6382	15.3638
Iteration 7	0	6.2919	9.6324	12.5293	10.6381	15.3637
Iteration 8	0	6.2920	9.6323	12.5292	10.6382	15.3639
Iteration 9	0	6.2919	9.6323	12.5292	10.6382	15.3639
Iteration 10	0	6.2919	9.6323	12.5292	10.6382	15.3639

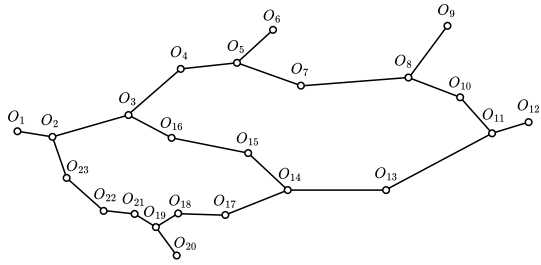

Figure 6. Second graph example with 23 nodes/vertices O_i and 24 edges e_j.

All values of F_i^ε were taken zero, except for $F_1^\varepsilon = -8\pi \cdot 10^{-16}$, $F_6^\varepsilon = 3 \cdot \pi \cdot 10^{-16}$, $F_9^\varepsilon = 1.5 \cdot \pi \cdot 10^{-16}$, $F_{12}^\varepsilon = 4 \cdot \pi \cdot 10^{-17}$ and $F_{20}^\varepsilon = 3 \cdot \pi \cdot 10^{-16}$. The iterative algorithm was used to acquire values of O_i, $i = 2, \ldots, 23$. The results are presented in the following Table 2.

7 Conclusions

The paper introduces and analyses the convergence of numerical methods to solve a nonlinear equation on the graph appearing in the modeling of non-Newtonian flows in thin tube structures. The real life rheology for the blood flow in a realistic network of blood vessels is simulated. In future, we intend to study numerically the influence of the choice of the parameter τ on the convergence rate and its optimization.

Table 2. Values of graph points O_i for the second example. The "Exact" column gives the solution found with MATLAB nonlinear equations solver *Fsolve*, while others present results acquired with the proposed iterative method. Here, equations were scaled by 10^{19} and the step size in artificial time was taken equal to 1/58.

	Exact	Iter. 1	Iter. 2	Iter. 3	Iter. 5	Iter. 10
O_1	0	0	0	0	0	0
O_2	0.0825	0.0856	0.0824	0.0829	0.0834	0.0834
O_3	0.1704	0.1641	0.1736	0.1699	0.1715	0.1715
O_4	0.2479	0.2253	0.2528	0.2473	0.2490	0.2491
O_5	0.3108	0.2750	0.3172	0.3102	0.3121	0.3121
O_6	0.3420	0.2994	0.3488	0.3414	0.3433	0.3433
O_7	0.3290	0.2819	0.3308	0.3272	0.3302	0.3303
O_8	0.3669	0.2963	0.3593	0.3625	0.3681	0.3684
O_9	0.3924	0.3126	0.3832	0.3878	0.3936	0.3939
O_{10}	0.3507	0.2858	0.3447	0.3470	0.3521	0.3523
O_{11}	0.3362	0.2763	0.3316	0.3330	0.3376	0.3379
O_{12}	0.3442	0.2798	0.3375	0.3401	0.3455	0.3459
O_{13}	0.2930	0.2467	0.2910	0.2906	0.2946	0.2948
O_{14}	0.2553	0.2207	0.2555	0.2535	0.2570	0.2572
O_{15}	0.2298	0.2037	0.2310	0.2284	0.2313	0.2315
O_{16}	0.1916	0.1783	0.1941	0.1908	0.1929	0.1929
O_{17}	0.2530	0.2197	0.2552	0.2527	0.2560	0.2562
O_{18}	0.2516	0.2190	0.2550	0.2523	0.2555	0.2556
O_{19}	0.2501	0.2183	0.2548	0.2517	0.2548	0.2549
O_{20}	0.2917	0.2508	0.2969	0.2933	0.2964	0.2966
O_{21}	0.2082	0.1852	0.2117	0.2095	0.2120	0.2120
O_{22}	0.1663	0.1520	0.1686	0.1673	0.1691	0.1691
O_{23}	0.1244	0.1188	0.1255	0.1251	0.1262	0.1262

Acknowledgements

This article has received funding from European Social Fund (project No 09.3.3-LMT-K-712-17-0003) under grant agreement with the Research Council of Lithuania (LMTLT).

References

[1] N. Bakhvalov. *Méthodes Numériques*. Editions Mir, Moscou, 1976.

[2] F. Blanc, O. Gipouloux, G. Panasenko and A.M. Zine. Asymptotic analysis and partial asymptotic decomposition of the domain for Stokes equation in tube structure. *Mathematical Models and Methods in Applied Sciences*, **9**(09):1351–1378, 1999. https://doi.org/10.1142/S0218202599000609.

[3] R. Bunoiu and A. Gaudiello. On the Bingham flow in a thin Y-like shaped structure. *J. Math. Fluid Mech.*, **24**:20, 2022. https://doi.org/10.1007/s00021-021-00657-0.

[4] R. Bunoiu, A. Gaudiello and A. Leopardi. Asymptotic analysis of a Bingham fluid in a thin T-like shaped structure. *J. Math. Pures Appl.*, **123**:148–166, 2019. https://doi.org/10.1016/j.matpur.2018.01.001.

[5] C. D'Angelo and A. Quarteroni. On the coupling of 1D and 3D diffusion-reaction equations: application to tissue perfusion problems. *Arch. Rat. Mech. Anal.*, **18**(08):1481–1504, 2008. https://doi.org/10.1142/S0218202508003108.

[6] T. Köppl, E. Vidotto and B. Wohlmuth. A 3D-1D coupled blood flow and oxygen transport model to generate microvascular networks. *Int. J. for Num. Meth. in Biomed. Eng.*, **36**(10):e3386, 2020. https://doi.org/10.1002/cnm.3386.

[7] V. Kozlov, S. Nazarov and G. Zavorokhin. A fractal graph model of capillary type systems. *Complex Variables and Elliptic Equations*, **63**(7-8):1044–1068, 2018. https://doi.org/10.1080/17476933.2017.1349117.

[8] B. Liu and D. Tang. Influence of non-Newtonian properties of blood on the wall shear stress in human atherosclerotic right coronary arteries. *Mol. Cell Biotech*, **8**(1):73–90, 2011.

[9] E. Marušić-Paloka and I. Pažanin. A note on Kirchhoff junction rule for power-law fluids. *Zeitschrift für Naturforschung A*, **70**(9):695–702, 2015. https://doi.org/10.1515/zna-2015-0148.

[10] C. Murray. The physiological principle of minimum work applied to the angle of branching of arteries. *J. Gen. Physiol.*, **9**(6):835–841, 1926. https://doi.org/10.1085/jgp.9.6.835.

[11] C. Murray. A relationship between circumference and weight in trees and its bearing on branching angles. *The Journal of general physiology*, **10**(5):725, 1927. https://doi.org/10.1085/jgp.10.5.725.

[12] D. Notaro, L. Cattaneo, L. Formaggia, A. Scotti and P. Zunino. *A mixed finite element method for modeling the fluid exchange between microcirculation and tissue interstitium*, pp. 3–25. Springer, 2016. https://doi.org/10.1007/978-3-319-41246-7_1.

[13] G. Panasenko. *Multi-scale Modeling for Structures and Composites*. Springer, Dordrecht, 2005.

[14] G. Panasenko. *Initiation à l'Analyse Numérique*. Editions Universitaires Européennes, Chisinau, Springer, Dordrecht, 2022.

[15] G. Panasenko and K. Pileckas. Asymptotic analysis of the nonsteady viscous flow with a given flow rate in a thin pipe. *C.R. Acad. Sci. Paris*, **326**(12):867–872, 1998.

[16] G. Panasenko and K. Pileckas. Asymptotic analysis of the nonsteady viscous flow with a given flow rate in a thin pipe. *Applicable Analysis*, **91**(3):559–574, 2012. https://doi.org/10.1080/00036811.2010.549483.

[17] G. Panasenko and K. Pileckas. Flows in a tube structure: equation on the graph. *Journal of Mathematical Physics*, **55**(8):081505, 2014. https://doi.org/10.1063/1.4891249.

[18] G. Panasenko and K. Pileckas. Asymptotic analysis of the non-steady Navier-Stokes equations in a tube structure. I. The case without boundary layer-in-time. *Nonlinear Analysis, Series A, Theory, Methods and Applications*, **122**:125–168, 2015. https://doi.org/10.1016/j.na.2015.03.008.

[19] G. Panasenko and K. Pileckas. Asymptotic analysis of the non-steady Navier-Stokes equations in a tube structure. II. General case. *Nonlinear Analysis, Series A, Theory, Methods and Applications*, **125**:582–607, 2015. https://doi.org/10.1016/j.na.2015.05.018.

[20] G. Panasenko and K. Pileckas. Periodic in time flow in thin structures: Equations on the graph. *Journal of Mathematical Analysis and Applications*, **490**(2):1–8, 2020. https://doi.org/10.1016/j.jmaa.2020.124335.

[21] G. Panasenko, K. Pileckas and B. Vernescu. Steady state non-Newtonian flow with strain rate dependent viscosity in domains with cylindrical outlets to infinity. *Nonlinear Analysis: Modeling and Controle*, **26**(6):1166–1199, 2021. https://doi.org/10.15388/namc.2021.26.24600.

[22] G. Panasenko, K. Pileckas and B. Vernescu. Steady state non-Newtonian flow in thin tube structure: equation on the graph. *St. Petersburg Mathematical Journal*, **33**:327–340, 2022. https://doi.org/10.1090/spmj/1702.

[23] G. Panasenko, K. Pileckas and B. Vernescu. Steady state non-Newtonian flow with strain rate dependent viscosity in thin tube structure with no slip boundary condition. *Mathematical Modeling of Natural Phenomena*, **17**(18):1–36, 2022. https://doi.org/10.1051/mmnp/2022005.

[24] C. Poelma. Exploring the potential of blood flow network data. *Meccanica*, **52**:489–502, 2017. https://doi.org/10.1007/s11012-015-0255-4.

[25] A.R. Pries, T.W. Secomb, T. Gessner, M.B. Sperandio, J.F. Gross and P. Gaehtgens. Resistance to blood flow in microvessels in vivo. *Circ. Res.*, **75**:904–915, 1994. https://doi.org/10.1161/01.RES.75.5.904.

[26] A. Quarteroni and F. Saleri. *Calcul Scientifique*. Springer-Verlag Italia, Milano, 2006.